

Production of Medical Radioisotopes with High Specific Activity in Photonuclear Reactions with γ Beams of High Intensity and Large Brilliance

D. Habs¹, and U. Köster²

¹ Fakultät für Physik, Ludwig Maximilians Universität München, D-85748 Garching, Germany

² Institut Laue Langevin, 6 rue Jules Horowitz, F-38042 Grenoble Cedex 9, France

Received: date / Revised version: date

Abstract We study the production of radioisotopes for nuclear medicine in $(\gamma, xn + yp)$ photonuclear reactions or (γ, γ') photoexcitation reactions with high flux $[(10^{13} - 10^{15})\gamma/s]$, small diameter $\sim (100\ \mu\text{m})^2$ and small band width $(\Delta E/E \approx 10^{-3} - 10^{-4})$ γ beams produced by Compton back-scattering of laser light from relativistic brilliant electron beams. We compare them to $(\text{ion}, xn + yp)$ reactions with $(\text{ion} = p, d, \alpha)$ from particle accelerators like cyclotrons and (n, γ) or (n, f) reactions from nuclear reactors. For photonuclear reactions with a narrow γ beam the energy deposition in the target can be managed by using a stack of thin target foils or wires, hence avoiding direct stopping of the Compton and pair electrons (positrons). However, for ions with a strong atomic stopping only a fraction of less than 10^{-2} leads to nuclear reactions resulting in a target heating, which is at least 10^5 times larger per produced radioactive ion and is often limits the achievable activity. In photonuclear reactions the well defined initial excitation energy of the compound nucleus leads to a small number of reaction channels and enables new combinations of target isotope and final radioisotope. The narrow bandwidth γ excitation may make use of the fine structure of the Pygmy Dipole Resonance (PDR) or fluctuations in γ -width leading to increased cross sections. Within a rather short period compared to the isotopic half-life, a target area of the order of $(100\ \mu\text{m})^2$ can be highly transmuted, resulting in a very high specific activity. (γ, γ') isomer production via specially selected γ cascades allows to produce high specific activity in multiple excitations, where no back-pumping of the isomer to the ground state occurs. We discuss in detail many specific radioisotopes for diagnostics and therapy applications. Photonuclear reactions with γ beams allow to produce certain radioisotopes, e.g. ^{47}Sc , ^{44}Ti , ^{67}Cu , ^{103}Pd , $^{117\text{m}}\text{Sn}$, ^{169}Er , $^{195\text{m}}\text{Pt}$ or ^{225}Ac , with higher specific activity and/or more economically than with classical methods. This will open the way for completely

new clinical applications of radioisotopes. For example $^{195\text{m}}\text{Pt}$ could be used to verify the patient's response to chemotherapy with platinum compounds before a complete treatment is performed. Also innovative isotopes like ^{47}Sc , ^{67}Cu and ^{225}Ac could be produced for the first time in sufficient quantities for large-scale application in targeted radionuclide therapy.

1 Introduction

In nuclear medicine radioisotopes are used for diagnostic and therapeutic purposes [1, 2]. Many diagnostics applications are based on molecular imaging methods, i.e. either on positron emitters for 3D imaging with PET (positron emission tomography) or gamma ray emitters for 2D imaging with planar gamma cameras or 3D imaging with SPECT (single photon emission computer tomography)¹. The main advantage of nuclear medicine methods is the high sensitivity of the detection systems that allows using tracers at extremely low concentrations (some pmol in total, injected in typical concentrations of nmol/l). This extremely low amount of radiotracers assures that they do not show any (bio-)chemical effect on the organism. Thus, the diagnostic procedure does

¹ Today the nuclear medicine imaging techniques PET and SPECT (using radionuclides injected into the patient's body) are frequently combined in the same apparatus with the radiology technique CT (computer tomography) to PET/CT or SPECT/CT, respectively. CT is based on transmission radiography with X-rays and provides structural information to better localize the features observed on PET or SPECT images. CT information helps also to perform the attenuation correction. However, the combination with CT, or not, does not affect the choice of the PET or SPECT tracer isotopes which is the main issue in the present discussion. Hence we use PET and SPECT, which implicitly includes CT where adequate.

not interfere with the normal body functions and provides direct information on the normal body function, not perturbed by the detection method. Moreover, even elements that would be chemically toxic in much higher concentrations can be safely used as radiotracers (e.g. thallium, arsenic, etc.). To maintain these intrinsic advantages of nuclear medicine diagnostics one has to assure that radiotracers of relatively high specific activity are used, i.e. that the injected radiotracer is not accompanied by too much stable isotopes of the same (or a chemically similar) element.

Radioisotopes are also used for therapeutic applications, in particular for endo-radiotherapy. Targeted systemic therapies allow fighting diseases that are non-localized, e.g. leukemia and other cancer types in an advanced state, when already multiple metastases have been created. Usually a bioconjugate [1] is used that shows a high affinity and selectivity to bind to peptide receptors or antigens that are overexpressed on certain cancer cells with respect to normal cells. Combining such a bioconjugate with a suitable radioisotope such as a (low-energy) electron or alpha emitter, allows irradiating and destroying selectively the cancer cells. Depending on the nature of the bioconjugate, these therapies are called Peptide Receptor Radio Therapy (PRRT) [2, 3] when peptides are used as bioconjugates or radioimmunotherapy (RIT) [2, ?], when antibodies are used as bioconjugates. Bioconjugates could also be antibody-fragments, nanoparticles, microparticles, etc. For cancer cells having only a limited number of selective binding sites, an increase of the concentration of the bioconjugates may lead to blocking of these sites and, hence, to a reduction in selectivity. Therefore the radioisotopes for labeling of the bioconjugates should have a high specific activity to minimize injection of bioconjugates labeled with stable isotopes that do not show radiotherapeutic efficiency. Thus often high specific activities are required for radioisotopes used in such therapies.

The tumor uptake of bioconjugates varies considerably from one patient to another. This leads to an important variation in dose delivered to the tumor if the same activity (or activity per body mass or activity per body surface) was administered. Ideally a personalized dosimetry should be performed by first injecting a small quantity of the bioconjugate in question, marked by an imaging isotope (preferentially β^+ emitter for PET). Thus the tumor uptake can be quantitatively determined and the injected activity of the therapy isotope can be adapted accordingly. To assure a representative in-vivo behaviour of the imaging agent, the PET tracer should be ideally an isotope of the same element as the therapy isotope, or, at least of a chemically very similar element such as neighboring lanthanides. Thus so-called “matched pairs” of diagnostic and therapy isotopes are of particular interest: $^{44}\text{Sc}/^{47}\text{Sc}$, ^{61}Cu or $^{64}\text{Cu}/^{67}\text{Cu}$, $^{86}\text{Y}/^{90}\text{Y}$, ^{123}I or $^{124}\text{I}/^{131}\text{I}$ or $^{152}\text{Tb}/^{149}\text{Tb}$ or ^{161}Tb . Often the production of one of these isotopes

is less straightforward with classical methods. Therefore “matched pairs” are not yet established as standard in clinical practice. The “matched pairs” of scandium and copper can be produced much better with γ beams. Valence-III elements do not necessarily show an identical in-vivo behaviour [5, 6] but in many cases they are sufficiently similar. For example the 68 min PET tracer ^{68}Ga is conveniently eluted from ^{68}Ge generators and used as imaging analog for the therapy isotopes ^{90}Y , ^{177}Lu or ^{213}Bi [7].

The radioisotopes for diagnostic or therapeutic nuclear medicine applications are usually produced by nuclear reactions. The required projectiles are typically either neutrons (from dedicated irradiation reactors) or charged particles (from small or medium-sized cyclotrons or other accelerators). In section 2 we shortly discuss these presently used techniques and then introduce in section 3 the new γ beams with high γ energies, high intensities and small bandwidth. Such a γ facility will typically consist of an electron linac, delivering a relativistic electron beam with high brilliance and high intensity from which intense laser beams are Compton back-scattered. These γ facilities allow to produce many radioisotopes in new photonuclear reactions with significantly higher specific activity. In section 4 we compare for certain radioisotopes of interest the specific activities achievable with presently used production reactions and γ -beams respectively. In section 5 the energy deposition of γ beams is compared to ion beams, showing that targets can endure higher intensities of γ beams than ion beams allowing for higher γ flux densities. We will discuss interesting cases of specific radioisotopes in section 6. Besides attaching radioisotopes to biomolecules in therapeutical applications, we discuss in section 7 new ways of brachytherapy. Finally in section 8 the advantages of producing radioisotopes by γ beams are outlined.

2 Presently used Nuclear Reactions to Produce Medical Radioisotopes

Today the most frequently employed nuclear reactions for the production of medical radioisotopes are:

1 Neutron capture

Neutron capture (n, γ) reactions transmute a stable isotope into a radioactive isotope of the same element. High specific activities are obtained, when the (n, γ) cross section is high and the target is irradiated in a high neutron flux. Neutrons most useful for (n, γ) reactions have energies from meV to keV (thermal and epithermal neutrons) and are provided in the irradiation positions of high flux reactors at flux densities of 10^{14} n/(cm²s) up to few 10^{15} n/(cm²s). If the neutron capture cross section is sufficiently high (e.g. 2100 barn for $^{176}\text{Lu}(n, \gamma)^{177}\text{Lu}$), then a good fraction of the target atoms can be transmuted to the desired

product isotopes, resulting in a product of high specific activity.

Note that the specific activity of the product depends on the neutron flux density ($n/(cm^2s)$) and not on the total number of neutrons provided by the reactor. Hence irradiation reactors are optimized to provide a high flux density in a limited volume, while keeping the total neutron rate (that is proportional to the thermal power) relatively low. This optimization is inverse to a power reactor that should provide a high thermal power at limited neutron flux density (to limit the power density, damage to structural materials and extend the operation time between refuelling).

High specific activities can also be achieved by using indirect production paths. The (n,γ) reaction is not populating directly the final product but a precursor that decays by beta decay to the final product. Thus the final product differs in its chemical properties from the target and can be chemically separated from the bulk of the remaining target material. This method is e.g. used to produce ^{177}Lu in non-carrier added quality by irradiating enriched ^{176}Yb targets in a high neutron flux to produce ^{177}Yb that subsequently decays to ^{177}Lu . The latter is extracted by a chemical Lu/Yb separation.

2 Nuclear fission

Fission is another process used for isotope production in nuclear reactors. Radiochemical separation leads to radioisotopes of “non-carrier-added” quality, with specific activity close to the theoretical maximum. Fission is the dominant production route for the generator isotopes ^{99}Mo and ^{90}Sr , for the β^- -emitting therapy isotope ^{131}I and for the SPECT isotope ^{133}Xe .

3 Charged particle reactions with p , d or α ions

Imaging for diagnostic purposes requires either β^+ emitters for PET (mainly ^{18}F , ^{11}C , ^{13}N , ^{15}O , ^{124}I or ^{64}Cu), or isotopes emitting gamma-rays with suitable energy for SPECT (about 70 to 300 keV), if possible without $\beta^{+/-}$ emission to minimize the dose to the patient. Thus electron capture decay is preferred for such applications, e.g.: ^{67}Ga , ^{111}In , ^{123}I , ^{201}Tl . Usually these neutron-deficient isotopes cannot be produced by neutron capture on a stable isotope (exception ^{64}Cu). Instead they are mainly produced by charged-particle induced reactions such as (p,n) , $(p,2n)$,... High specific activities of the final product are achievable, when the product differs in chemical properties from the target (i.e. different Z) and can be chemically separated from the remaining bulk of target material². Thus Z must be changed in the nuclear reaction, e.g. in (p,n) , $(p,2n)$, (p,α) reac-

tions. The energies of the charged particle beams for such reactions are usually in the range of 10 to 30 MeV and can be supplied with high currents (0.1 to 1 mA) by small cyclotrons.

Table 1 Radioisotopes for nuclear medicine produced in generators. *: ^{212}Pb and ^{213}Bi are the grand-grand-daughters and ^{212}Bi is the grand-grand-grand-daughter of the respective generator isotope.

mother isotope	$T_{1/2}$	daughter isotope	$T_{1/2}$
^{44}Ti	60.4 a	^{44}Sc	3.9 h
^{52}Fe	8.3 h	^{52}Mn	21 m
^{68}Ge	288 d	^{68}Ga	68 m
^{81}Rb	4.6 h	^{81}Kr	13 s
^{82}Sr	25.0 d	^{82}Rb	76 s
^{90}Sr	28.5 a	^{90}Y	64 h
^{99}Mo	66 h	^{99m}Tc	6.0 h
^{188}W	69 d	^{188}Re	17 h
^{224}Ra	3.7 d	$^{212}Pb^*$	10.6 h
^{224}Ra	3.7 d	$^{212}Bi^*$	61 m
^{225}Ac	10 d	$^{213}Bi^*$	45 m

4 Generators

Another important technique is the use of generators, where short-lived radionuclides are extracted “on-tap” from longer-lived mother nuclides. Here the primary radioisotope (that was produced in the nuclear reaction) has a longer half-life than the final radioisotope (that is populated by decay of the primary radioisotope and is used in the medical application). The primary radioisotope is loaded onto the generator and stays there chemically fixed. The final radioisotope will grow in, populated by the decay of the primary radioisotope. It can be repetitively eluted and used. For the extraction of the shorter-lived isotope chromatographic techniques, distillation or phase partitioning are used. Depending on the generator technology, there is usually a limit to which a generator can be loaded with atoms of the primary product element (e.g. molybdenum on acid alumina columns). If more is loaded, then a significant part of the primary product isotope might be eluted too (“breakthrough”), leading to an unacceptable contamination of the product with long-lived activity. To prevent such problems, generators are generally loaded with material of a given minimum specific activity.

5 Photonuclear reactions

The inverse process to (n,γ) , namely (γ,n) , also al-

² Note that in principle very high specific activities may be achieved in this way. However, the effective specific activities that measure the ratio between wanted radioisotopes to all elements (mostly metals) that may affect, e.g., the labeling of

bioconjugates, might be significantly lower since stable elements can be introduced due to the finite purity of chemicals, columns, etc. used in the chemical processing. Such problems are generally reduced when higher activities per batch are processed.

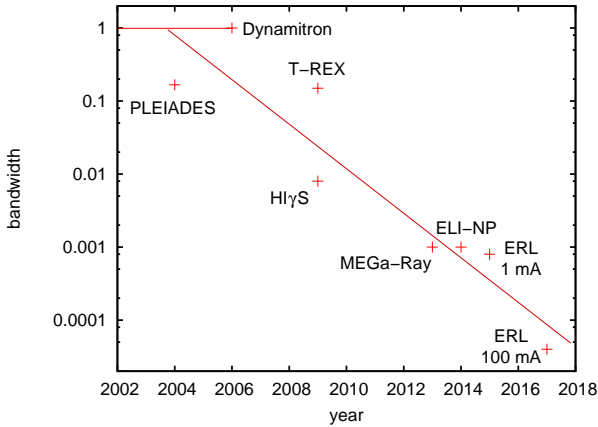


Fig. 1 Bandwidth of high energy γ beams (≈ 10 MeV) as a function of time.

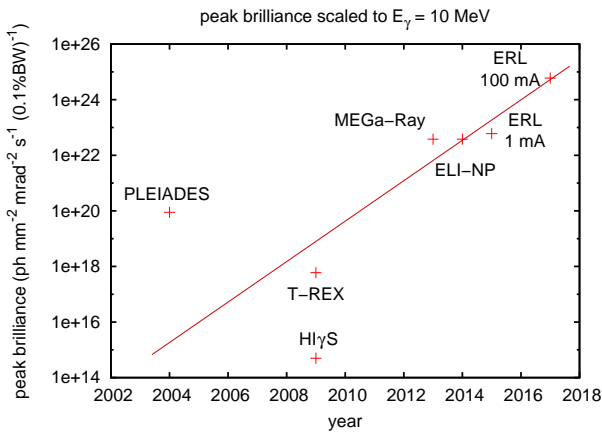


Fig. 2 Peak brilliance of high energy γ beams (≈ 10 MeV) as a function of time.

lows producing neutron deficient isotopes, but conventional γ ray sources do not provide sufficient flux density for efficient production of radioisotopes with high total activity and high specific activity. Therefore this process plays no role in present radioisotope supply.

3 γ Beams

The new concept of isotope production with a γ beam only became possible, because very brilliant γ sources are being developed, where the γ rays are produced by incoherent Compton back-scattering of laser light from brilliant high-energy electron bunches. Fig. 1 and Fig. 2 show the rapid progress of γ beam properties for the bandwidth (Fig. 1) and the peak brilliance (Fig. 2) with time, starting with the bremsstrahlung spectrum of the Stuttgart Dynamitron [8], which still had a very large bandwidth.

For Compton back-scattering in a head-on collision the γ energy is given by:

$$E_\gamma = \frac{4\gamma_e^2 E_L}{1 + (\gamma_e \Theta_\gamma)^2 + 4\gamma_e E_L / mc^2} \quad (1)$$

with the γ_e factor, characterizing the energy of the electron beam, the γ energy E_γ , its angle Θ_γ and the laser photon energy E_L . The energy E_γ decreases with Θ_γ . A small bandwidth of the γ beam requires a small energy spread of the electron bunches ($\Delta\gamma_e/\gamma_e$), a small bandwidth of the laser energy ($\Delta E_L/E_L$), a very good emittance of the electron beam with a small opening angle and small opening angle of the laser beam. At the HI γ S facility (Duke University, USA) the photons are produced by a Free Electron Laser (FEL) and then are back-scattered from a circulating electron beam [9]. This facility already produced high energy γ rays (1-100 MeV), but the flux ($10^5 - 5 \cdot 10^8 \gamma/s$) was too weak for radioisotope production. C. Barty and his group at the Lawrence Livermore National Laboratory (LLNL) developed already three generations of incoherent Compton back-scattering sources: PLEIADES [10], T-REX [11] and MEGa-Ray [12], each based on a “warm” electron linac and a fibre laser for back-scattering. Recently the electron linac technology was switched from S-band technology (4 GHz) for T-REX to X-band technology (12 GHz) for MEGa-Ray. Here electron bunches with 250 pC are used. The MEGa-Ray γ beam runs with a macropulse structure of 120 Hz using 1.5 J, 2 ps laser pulses, which are recirculated 100 times with 2 ns bunch spacing in a ring-down cavity. The group plans for lower energy γ rays in the range of a only few MeV, too small for photonuclear reactions. A similar γ facility is planned for the ELI-Nuclear Physics project (ELI-NP) in Romania [13], also based on a “warm” linac like the one used at MEGa-Ray, however designed for γ energies up to 19 MeV, thus reaching interesting intensities and γ energies for isotope production. R. Hajima and coworkers at Ibaraki (Japan) are developing a Compton back-scattering γ beam using an energy recovery linac (ERL) and superconducting “cold” cavities [14]. For smaller electron bunch charges (8 pC) very low normalized emittances of 0.1 mm mrad can be obtained from the electron gun. For the reflected laser light a high finesse enhancement cavity is used for recirculating the photons. The quality of the electron beam from the ERL can be preserved by running with higher repetition rate (GHz). Switching from a 1 mA electron current to a 100 mA current the peak brilliance and bandwidth can be improved significantly [15,16]. Intensities of $5 \cdot 10^{15} \gamma/s$ are expected [15].

Also laser-accelerated electron bunches have been proposed as relativistic mirrors for Compton back-scattering and the production of intense γ beams [17].

The yield of resonant photonuclear reactions (discussed below) depends strongly on the exact energy and the bandwidth of the gamma beam. Both parameters are determined by the quality of the laser beam and of the electron beam respectively. The laser beam parameters are usually well controlled by conventional means used in

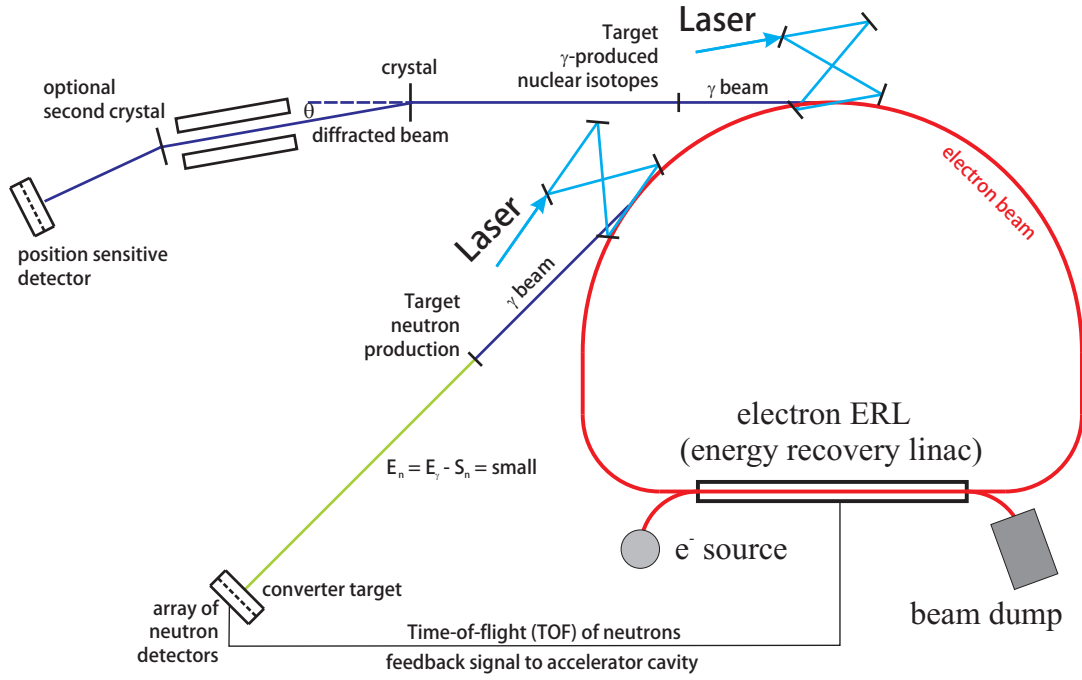


Fig. 3 Energy Recovery Linac (ERL) electron beam facility with 2 γ -beam production points and a crystal spectrometer and neutron time of flight (TOF) spectrometer to monitor the γ energy. The electron beam starts from the electron source, is accelerated in the superconducting cavity and then, after one loop, is decelerated again in the same cavity, feeding back its energy, and then is stopped in the beam dump. For Compton back-scattering the laser light is recycled many times in the enhancement cavity.

laser spectroscopy. More importantly, the electron beam parameters need to be tuned and monitored with good precision. For a meaningful monitoring system the γ ray energy has to be measured with a system that has (far) better energy resolution than the γ beam itself. It is not trivial to measure high energy gamma ray energies with such high precision. For gamma rays in the MeV range usual Ge detectors are limited to an energy resolution of the order of 10^{-3} . Scintillation detectors have an even worse energy resolution. Hence, more complex and “unusual” methods have to be used for this purpose. The two methods are shown schematically in Fig. 3, where an energy recovery linac can supply many γ beams.

Two methods are preferable:

A crystal spectrometer A thin single or mosaic crystal (e.g. Si, Ge, SiO₂, Cu, graphite, etc.) is placed in the gamma beam (in front, inside or behind a production target). A small fraction of the beam will be diffracted by the crystal according to the Bragg condition:

$$2d \sin \theta = n\lambda \quad (2)$$

d is the well-known crystal lattice spacing, n is the reflection order, λ is the wavelength of the γ beam and θ is the diffraction angle. Placing a γ ray detection system at large distance allows measuring the diffraction angle θ , either by scanning the beam through narrow collimators by turning the crystal or by using a fixed crystal and a detector with good position resolution. Hence, the wavelength of the γ rays is

deduced which gives directly the γ ray energy. The angular spread of the diffracted beam is a measure of the energy spread of the γ beam. These data can be used for a feedback system for tuning and monitoring the electron beam for the γ beam production. Due to the high intensity of the γ beam, even with thin crystals and in high reflection order enough photons will arrive at the detector. A higher reflection order is preferred since it allows placing the detector further away from the direct non-diffracted beam. For γ beams of larger opening angle, the latter would limit the achievable energy resolution. Here it is preferable to use two consecutive crystals for diffraction: a first one placed in the γ beam to diffract out a small fraction. The small intrinsic angular acceptance of the crystal will effectively act as collimator. The second crystal receives therefore a well-collimated beam. Additional collimators can be placed between both crystals and/or between the second crystal and the detector respectively to eliminate background from other diffraction orders. Using two consecutive diffractions in the same direction will add to the energy dispersion and provide very high energy resolution, two diffractions in opposite direction allows measuring the intrinsic resolution of the measurement system. The rotation angle of the crystals is usually controlled by laser interferometers. Such a double crystal spectrometer enables measuring γ ray energies with a resolution below 10^{-6} [18], i.e. covering fully the

needs to stabilize the γ beam in a bandwidth of 10^{-5} to 10^{-3} .

B (γ, n) threshold reaction with neutron time-of-flight spectrometer

Alternatively to a crystal spectrometer also a second γ beam from a second γ ray production station (possibly using a different laser wavelength) can be used for monitoring the electron beam energy. This second γ beam is sent on a dedicated target where it induces (γ, n) reactions just above the threshold and neutrons are released in the eV to keV range. Due to the pulsed nature of the γ beam, the neutron energy can be measured by time-of-flight with good precision (few eV or better). Adding the measured neutron energy to the well-known neutron binding energy of the target provides an accurate on-line measurement (order of 10^{-6} resolution) of the γ beam energy and γ beam energy spread, hence also of the electron beam energy and electron beam energy spread. Again this information is used for a feedback system to optimize and stabilize the electron accelerator parameters. Neutron detection can be realized in various way. One possibility is the use of a “neutron converter” (containing isotopes like ^6Li , ^{10}B or ^{235}U) combined with a charged particle detector. Using a segmented detector array many neutrons could be measured per bunch allowing for a fast feedback system. The length of the neutron flight path should be adjusted to the neutron energies.

4 Specific Activity of Radioisotopes and Photonuclear Cross Sections

One of the most important quality criteria for radioisotopes for nuclear medicine applications is the specific activity (A/m), usually expressed in GBq/mg, Ci/mg or similar units. The theoretical maximum specific activity for a pure radioisotope without admixture of stable isotopes is given by:

$$\left(\frac{A}{m}\right)_{\max} = \frac{\ln(2) \cdot N_A}{T_{1/2} \cdot M} \quad (3)$$

Where $T_{1/2}$ is the half-life of the radioactive isotope, M is the molar mass (g/mol) of the target isotope and $N_A = 6.02 \cdot 10^{23}$ denotes Avogadro’s constant.

For example an isotope with $M = 100$ g/mol and $T_{1/2} = 7$ days would have a theoretical specific activity of nearly 7 TBq/mg.

If other reactions (such as destruction of the product by nuclear reactions) do not interfere significantly, then the achievable specific activity is given by:

$$\frac{A}{m} = \frac{N_A}{M} \sigma \cdot \Phi \cdot [1 - \exp(-\ln(2)t_{\text{irr}}/T_{1/2})] \quad (4)$$

Where:

M	the molar mass of the target isotope
σ	the cross-section for transmutation of the target into the product
Φ	the particle flux density
t_{irr}	the irradiation time
$T_{1/2}$	the half-life of the product isotope

After sufficiently long irradiation (multiple of product half-life) the specific activity approaches saturation:

$$\frac{A}{m} = \frac{N_A}{M} \sigma \cdot \Phi \quad (5)$$

Comparison of equations 3 and 5 shows that the necessary condition to reach high specific activities is: $\sigma \cdot \Phi \approx \ln(2)/T_{1/2}$

Radioisotopes for medical applications have typically half-lives of hours to days, hence the flux density (in part./ (cm^2s)) should approach or exceed a value of about $10^{19}/\sigma$ (in barn). For future planned γ beams with $5 \cdot 10^{15} \gamma/\text{s}$ over areas of $(0.1 \text{ mm})^2$ the flux density can reach several $10^{19} \gamma/(\text{cm}^2 \text{ s})$, i.e. the target can be efficiently transmuted by photonuclear reactions with few 100 mb cross-section. For resonant reactions with higher cross-sections even the flux densities of the less powerful γ beam facilities ($10^{17} \gamma/(\text{cm}^2 \text{ s})$) will assure a relatively high specific activity of the product.

The specific activity of a radioisotope product in units of GBq/mg or Ci/mg is a measure of quality familiar to the users in nuclear medicine. However, the theoretical specific activity varies with the half-life. Hence a tabulation of different isotopes and their achievable specific activities is less comprehensible. Therefore we define in addition the ratio $R = [(A/m)/(A/m)_{\max}]$ that indicates how close the specific activity comes to the theoretical optimum. For $R = 0.5$ one radioactive atom will be accompanied by one stable atom (of the same element or target, respectively), for $R = 0.1$ only one out of ten atoms is the radioisotope of interest, etc.

We will compare $R_{(n,\gamma)} = [(A/m)/(A/m)_{\max}]_{(n,\gamma)}$ for classical production in (n,γ) reactions to $R_{\gamma} = [(A/m)/(A/m)_{\max}]_{\gamma}$ for γ -beams.

The finally reached specific activity is also determined by the undesired further transmutation (burnup) of the wanted reaction product. This product burnup becomes significant when the product fraction gets high. For (n,γ) reactions in high flux reactors it may eventually limit the achievable specific activity if the neutron capture cross-section of the product is high. For ^{153}Gd , ^{159}Dy , ^{169}Yb or ^{195m}Pt this seriously limits the achievable specific activity. For photonuclear reactions the cross sections for product creation and destruction are comparable in case of (γ, n) reactions, while for (γ, p) and ($\gamma, 2n$) reactions the destruction cross-section may be up to one order of magnitude larger. This limits the ultimately achievable specific activity to $R \approx 0.5$ in the first case and to $R \approx 0.1$ in the latter cases. Product burnup becomes noticeable when approaching these lim-

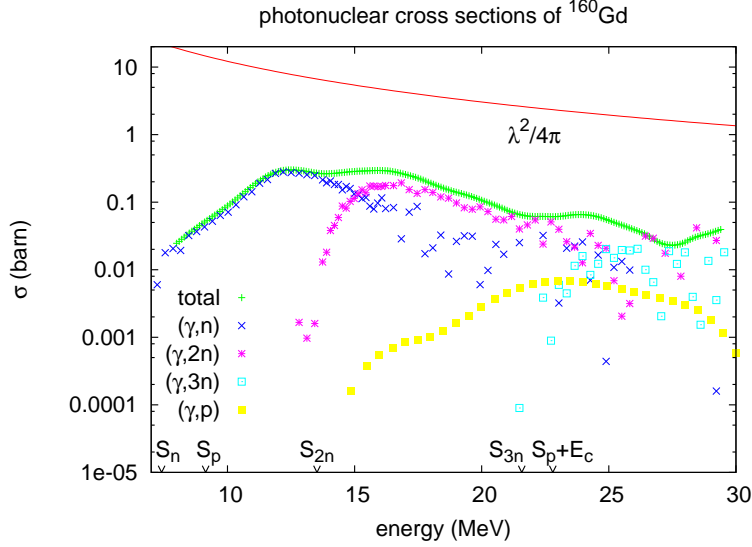


Fig. 4 Measured photonuclear cross section for ^{160}Gd . Also shown is the maximum Breit-Wigner resonance cross section $\frac{\lambda^2}{4\pi}$ as an orange curve. The threshold values for the reactions are indicated by arrows as well as the energy $S_p + E_c$ where Coulomb hindrance of proton emission disappears. The data are taken from Ref. [19].

its. If the cross-sections were known, the effect could be calculated precisely by the Bateman equations.

In some cases a secondary product produced by a reaction on the primary desired product may present a disturbing radionuclide impurity. For example when ^{125}I is produced by $^{124}\text{Xe}(\gamma, n)^{125}\text{Xe}(\beta^-)$, then the irradiation should be kept short enough to minimize production of disturbing ^{126}I by $^{125}\text{I}(n, \gamma)$ reactions.

If one looks at measured photonuclear cross-sections one typically finds cross sections below 1 barn. As a prototype we show in Fig. 4 the photonuclear cross-sections for ^{160}Gd . The arrows with separation energies indicate the thresholds for the $(\gamma, xn+yp)$ reactions. Close to threshold a transmission factor of the neutron and the proton reduces the cross-section. The protons in addition have a reduction by a Coulomb tunneling factor $\exp\left(-\frac{\pi(Z-1)e^2}{\hbar v}\right)$ with the velocity v of the proton and the charge Z of the nucleus, where Coulomb hindrance prevails up to the Coulomb energy $E_c = \frac{(Z-1)^2 e^2}{R}$ with the nuclear radius R . The exponential rise of the starting (γ, xn) reaction cross-sections is due to the increase in compound nucleus resonance level density.

If we could look with higher resolution into the photonuclear cross-sections, we would observe individual resonances characterized by a width Γ . The cross-section for a compound nucleus resonance of the (γ, x) reaction at the resonance energy E_r is given by the Breit-Wigner formula [20]:

$$\sigma(E_\gamma) = (\lambda_\gamma^2/4\pi) \cdot g \cdot \frac{\Gamma_\gamma \Gamma_d}{(E_\gamma - E_r)^2 + (\Gamma)^2/4} \quad (6)$$

g is a spin factor close to unity. $\lambda_\gamma = \hbar/(E_\gamma \cdot c)$ represents the wavelength of the γ rays with energy E_γ .

Γ is the total width of the resonance with $\Gamma = \Gamma_\gamma + \Gamma_d + \Gamma_D$ and the decay widths Γ_d to the desired product and Γ_D to all other exit channels. Γ_D may become important for less favored reactions like (γ, p) .

The width Γ_γ has been studied systematically as a function of A at the neutron separation energy [20] and we obtain an average $\Gamma_\gamma \approx 100$ meV for nuclei with $A = 160$. Frequently the integrated cross-section, i.e. the product of cross-section times the width Γ is given, which in our case is about 2 b-eV.

The energy spacing of the compound nuclear resonances for a given spin and parity at the neutron binding energy for $A = 160$ is about $D \approx 10$ eV [20]. It can be calculated from the back-shifted Fermi-gas formula [21]. Thus with $\Gamma/D \approx 1\%$ probability we hit a resonance. In Fig. 5 we show these Breit-Wigner resonances.

For a given γ beam energy of 7 MeV, a bandwidth $\Delta E \approx 7$ keV will cover about 700 resonances. The width Γ_γ , where we have shown the average in Fig. 4, has a Porter-Thomas distribution [22,23]

$$P(s) = \frac{1}{\sqrt{2\pi s}} \cdot \exp(-s/2). \quad (7)$$

with $s = \Gamma_\gamma / \langle \Gamma_\gamma \rangle$. So most of the resonances have a very small γ width and very few levels show a much larger width. Thus from energy bin to energy bin we expect large fluctuations of the average value within the bin and we can select an energy bin with a large cross section. The smaller the bandwidth of the γ -beam, the larger these fluctuations become and one may select e.g. bins with 10 times larger average cross section. Since the level spacings D grow exponentially when reducing the mass number A at the same excitation energy, these fluctuations become more pronounced for lighter nuclei.

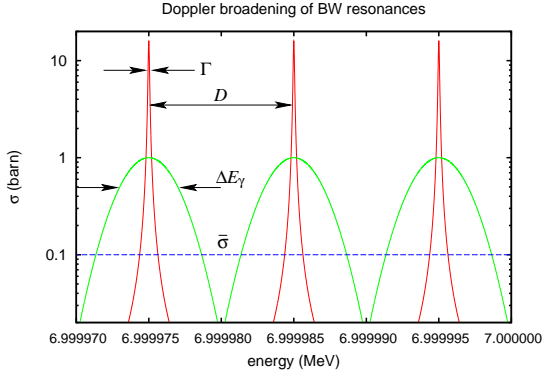


Fig. 5 Breit-Wigner cross sections (red), Breit-Wigner cross section broadened by the Doppler effect (green) and the energy averaged cross sections (dashed blue), showing the much larger individual resonance cross sections.

The Doppler broadening of a γ transition at room temperature $kT = 1/40$ eV for a nucleus with mass number $A = 160$ and a γ energy $E_\gamma = 7$ MeV is

$$\Delta E_\gamma = E_\gamma \sqrt{(2kT)/m_u c^2 A} \approx 4 \text{ eV} \quad (8)$$

Thus the line is broadened with respect to the natural linewidth by a factor of ≈ 40 .

Here the spectral flux density $\Phi/(\Delta E)$ is an important quantity, where we will reach values of $10^{13} \gamma/(\text{cm}^2 \cdot \text{s} \cdot \text{eV})$ at ELI-NP, but up to $10^{17} \gamma/(\text{cm}^2 \cdot \text{s} \cdot \text{eV})$ in Compton back-scattering with energy recovery electron linacs. The specific activity at saturation can then be calculated by multiplying the integrated cross-section $\sigma(E_r) \cdot \Gamma$ with the probability to hit a resonance and the spectral flux density:

$$\frac{A}{m} = \frac{N_A}{M} [\sigma(E_r) \cdot \Gamma] \frac{\Gamma}{D} \cdot \left(\frac{\Phi}{\Delta E} \right) \quad (9)$$

5 Comparison of the Energy Loss in the Target between Photonuclear and Ion-induced Reactions

Gamma rays deposit their energy in quantized interactions with matter, such as Compton scattering, pair creation, photo effect or photonuclear reactions. For photon energies between 10 and 30 MeV, the total cross-section is dominated by Compton scattering and pair production in the nuclear field. The dependence of the cross sections as a function of γ energy and target element is given in Ref. [24]. The Compton cross-section rises proportionally to the number of electrons per atom, i.e. to Z , while the cross-section for pair production rises roughly with Z^2 . At 15 MeV γ energy we find for carbon a total cross section of 0.34 b/atom, while for lead this value amounts to 20 b/atom. Generally the cross section is rather flat in this energy region. While for carbon the Compton cross-section is twice the pair creation cross section, for lead

the pair creation is five times more important than the Compton effect.

For 10 MeV γ quanta the angle of the Compton scattered γ 's is confined to about 10 degrees and the cross-section is strongly peaked in forward direction with an energy loss of less than 300 keV. If we assume a typical total cross-section of 10 b/atom and a target thickness of 10^6 atomic layers, about 5% of the γ quanta will suffer an energy loss by Compton scattering of 100 keV and about 5% will undergo pair creation at 10 MeV. However, in such thin targets of less than 0.1 g/cm² less than 10^{-2} of the electrons are stopped and less than $5 \cdot 10^{-5}$ of the energy is deposited.

In contrast to gamma rays, charged particles deposit their energy continuously while being slowed down in matter. The mean rate of energy loss is given in units of (MeV/(g/cm²)) (stopping power) by the Bethe-Bloch equation:

$$-\frac{dE}{dx} = K z^2 \frac{Z}{A} \frac{1}{\beta^2} \left[\frac{1}{2} \ln \frac{2m_e c^2 \beta^2 \gamma^2 T_{\max}}{I^2} - \beta^2 - \frac{\delta}{2} \right] \quad (10)$$

with $K = 4\pi N_A r_e^2 m_e c^2 = 0.307 \text{ MeV cm}^2$. Here T_{\max} is the maximum kinetic energy, which can be transferred in a single collision, Z the atomic number of the target, A the atomic number of the target, ze the charge of the ion and δ a density effect correction to the ionization energy loss. For 10 MeV protons we obtain 30 MeV/(g/cm²). Therefore with the density of iron of 7.9 g/cm³ we have an energy loss of 10 MeV in 0.26 mm. In these $2.6 \cdot 10^6$ atomic layers at Å distances, about 10^{-8} reactions occur per atomic layer or 2.6% in total. Thus we deposit per produced new radioactive nucleus about 400 MeV. The energy deposition is about a factor of 10^5 larger for protons compared to γ 's for the same number of produced nuclei.

The typical intensity of proton beams used for isotope production is of the order of 100 $\mu\text{A}/\text{cm}^2$, corresponding to $6 \cdot 10^{14}/(\text{cm}^2 \cdot \text{s})$. On the other hand, the target should withstand a higher γ flux density of $10^{19}/(\text{cm}^2 \cdot \text{s})$. However, for Bremsstrahlung beams one has a strong rise of the γ ray spectrum to low energies with increased energy deposition at lower energies, making it worse compared to proton activation.

6 Specific Radioisotopes produced in Photonuclear Reactions

We now discuss in detail the different γ -induced reactions and specific radioisotopes that can be produced by such reactions.

In tables 2 and 3 we show estimates of the achievable specific activities for thin targets for a γ flux of 10^{14} per s, corresponding to a flux density of $10^{18} \gamma/(\text{cm}^2 \cdot \text{s})$. With a bandwidth of 10^{-3} this results at 10 MeV in a spectral flux density of $10^{14} \gamma/(\text{cm}^2 \cdot \text{s} \cdot \text{eV})$. These

values are inbetween the characteristics of presently built facilities (e.g. MEGa-RAY) and future improved facilities (100 mA ERL). We compare these to thin target yields obtained by thermal neutron capture in a typical flux density of 10^{14} n/(cm² s) in high flux reactors. Note that alike for the potential beam parameters of γ beam facilities, there is also a wide range for the flux density really available at the irradiation positions of high flux reactors. Some positions provide flux densities of several 10^{12} to 10^{13} n/(cm² s), while few special reactors have positions that even exceed 10^{15} n/(cm² s), namely SM3 in Dimitrovgrad [25], HFIR in Oak Ridge [26] and ILL's high flux reactor in Grenoble.

Since hitherto no γ beams with sufficiently small bandwidth were available to exploit resonant excitation, there are obviously no such measured cross-sections. Hence, we can only estimate a lower bound using the averaged cross-sections measured at Bremsstrahlung facilities [19,27,29,28,30]. For cases where no measured cross-sections are available, we interpolate experimental cross-sections of the same reaction channel on nearby elements, taking into account the energy above the reaction threshold.

Even when using these conservative assumptions, the estimated specific activities are very promising for specific isotopes.

The total activity in a nuclear reactor can be relatively high since thick (several cm) and large (several cm²) targets can be used if the cross-sections are not too high (leading to self absorption and local flux depression). Multiple irradiation positions allow producing various radioisotopes with activities of many TBq.

For the γ beam we estimate the total activities by integrating to one interaction length, i.e. where the initial γ -beam intensity has dropped to $1/e = 37\%$ of its intensity. Higher total activities can be achieved with thicker targets at the expense of lower specific activity and vice versa. The total interaction cross-section is usually dominated by the atomic processes of Compton effect and pair creation. We consider conservatively any interacted γ ray as lost. In reality, part of the Compton scattering goes forward under small angles and the γ rays that have lost little energy can still induce photonuclear reactions. The usable target thickness ranges from 20 g/cm² for heavy elements to 40 g/cm² for light elements, i.e. in total only few mg target material are exposed to the small area of the γ beam. With non-resonant reactions of the order of 0.1 TBq activity can be produced per day, corresponding to tens (for β^- therapy isotopes) to thousands (for imaging isotopes and therapy with alpha emitters) of patient doses.

We consider metallic targets, although in praxi for certain elements rather chemical compounds would be used as targets. Usually oxides or other compounds with light elements are used. These light elements have a relatively low cross-section for gamma rays, hence the

specific activity achieved with compound targets is not much lower compared to elemental targets.

The exact target geometry does not affect our estimates. In principle a single compact target or a stack of thin target foils could be used and would provide similar production rates. In practice the latter solution can stand far higher beam intensities. The foils could be radiation-cooled in vacuum or helium-cooled, since helium has a low Z and correspondingly low cross section for interaction with gamma rays. Due to the low divergence of the γ beam, the individual target foils can be spaced wide apart, thus reducing the view factors between the foils to minimize mutual heating by radiation absorption. For sufficiently thin foils most of the forward-directed Compton and pair electrons and positrons can leave the foil. Spacing the foils further apart reduces the energy deposition from electrons of the previous foil, which deposit their energy laterally (e.g. in a water-cooled target chamber) spread over a wide area. The trajectories of the electrons and positrons could even be forced outward by applying transversal magnetic fields. Also a stack of target foils with thin water-cooling channels in between can be considered since hydrogen and oxygen have much lower interaction cross-sections with gamma rays.

Alternatively to thin foils also a thin wire (e.g. 0.1 mm diameter) or several consecutive wires could be placed along the γ beam direction. Here most electrons and positrons that are emitted under angles different from 0 degree will rapidly leave the target and not contribute much to its heating. Even those that are initially emitted forward will rapidly change direction by scattering and then leave the wire. In particular for less intense γ beams such a solution may be simpler to realize than a multi-foil stack.

All these heat dissipation techniques rely on the small area, small divergence and small bandwidth of a γ beam. They could not be applied for Bremsstrahlung spectra. Thus, the extremely high flux densities of γ beams can really be utilized without being seriously limited by the required heat dissipation from the targets as is frequently the case for charged-particle induced reactions or intense Bremsstrahlung spectra.

Instead of producing a single product isotope at a time, the target stack could also consist of different targets for simultaneous production of different isotopes. This is possible when the different reactions require similar γ energies. It may be particularly efficient when at least one of the reactions is characterized by prominent resonances, reducing the interaction length for resonant γ rays. The "unused" γ rays within the bandwidth of the γ beam may then be used downstream for other reactions that are not resonant or have resonances at different energies.

Table 2 Longer-lived nuclear isomers produced in (γ, γ') reactions. The relative population of the respective isomer in thermal neutron capture on $A-1$ target isotopes is given as I_{is}/I_{gs} where known experimentally. Experimental integrated cross sections for population of the isomer by (γ, γ') reactions at 4 MeV and 6 MeV were taken from [29,28]. The fraction of the maximum specific activity produced in (γ, γ') reactions R_γ , is put in relation to that obtained with (n, γ) reactions $R_{(n, \gamma)}$ at a thermal neutron flux of 10^{14} n./(cm^2 s) in the last column.

Iso- tope	Isomer			I_{is}/I_{gs}	Ground state		$\sigma \cdot \Gamma$		Spec. act. γ beam GBq/mg	Activity per day GBq	R_γ fraction of max.	Spec. act. high flux reactor GBq/mg	$R_\gamma/R_{(n, \gamma)}$
	Exc. energy keV	Spin & parity	$T_{1/2}$ d		Spin & parity	Nat. abun. %	at 4 MeV eV·b	at 6 MeV eV·b					
^{87}Sr	389	$1/2^-$	0.12	3.5	$9/2^+$	7	3.9	8.7	10	110	$2 \cdot 10^{-5}$	0.57	18
^{115}In	336	$1/2^-$	0.19		$9/2^+$	95.7	18	67	58	603	$3 \cdot 10^{-4}$		
^{117}Sn	315	$11/2^-$	13.8	0.04	$1/2^+$	7.68	3.2	8.8	7.5	0.6	0.0025	0.003	2400
^{119}Sn	90	$11/2^-$	293	0.02	$1/2^+$	8.59						0.002	
^{123}Te	248	$11/2^-$	119	0.13	$1/2^+$	0.89	42	68	55	0.6	0.17	0.2	280
^{125}Te	145	$11/2^-$	57.4	0.17	$1/2^+$	7.07	70				0.08	0.48	
^{129}Xe	236	$11/2^-$	8.9	0.10	$1/2^+$	26.4						0.2	
^{131}Xe	164	$11/2^-$	11.8	0.10	$3/2^+$	21.2						0.2	
^{135}Ba	268	$11/2^-$	1.2	0.08	$3/2^+$	6.59	13	60	44	33	$1.5 \cdot 10^{-3}$	0.045	1000
^{176}Lu	123	1^-	0.15	2.0	7^-	2.59	140	350	2.0	1800	$1.2 \cdot 10^{-3}$	5.5	36
^{180}Hf	1141	8^-	0.23	0.01	0^+	35.1						0.14	
^{193}Ir	80	$11/2^-$	10.5		$3/2^+$	62.7					10^{-5}		
^{195}Pt	259	$13/2^+$	4.02	0.09	$1/2^-$	33.8	30	140	72	17	0.012	0.019	3800

6.1 Isomers of stable isotopes via (γ, γ') reactions

Longer-lived nuclear isomers that decay by emission of gamma rays and/or conversion electrons to the respective ground state are of interest for various applications in nuclear medicine if they can be produced with high specific activity. Table 2 shows a selection of such isomers. The table shows in addition also other isomers that have at present no application in nuclear medicine, but are of interest e.g. for Mößbauer spectroscopy or even gamma-ray lasers.

Most usual production methods, e.g. via (n, γ) reactions, result in relatively low specific activity since the dominant part of the production proceeds directly to the nuclear ground state that has a nuclear spin closer to that of the $A-1$ target isotope. However, the fact that all these isomers are actually populated via thermal neutron capture reactions on low-spin $A-1$ target isotopes proves that pathways populating the high-spin isomers from higher-lying, low-spin compound nucleus resonances levels of lower spins must exist. In Ref. [31] the population of high-spin isomers relative to the ground state was studied for resonances in (n, γ) reactions. An energy dependence of the isomeric ratio was observed. One may expect that this energy dependence would become even more pronounced if the reactions were excited with a primary beam of smaller bandwidth that populates more selectively states which decay mainly to the isomeric level of interest.

Also photoexcitation (γ, γ') experiments with Bremsstrahlung beams were performed on a series of stable targets and showed strong population of isomeric levels

[27,29,30]. The observed energy dependence of the isomer activation yields indicates that few gateway states are responsible for populating efficiently the isomers.

It was recently demonstrated that Coulomb excitation to states communicating by gamma transitions with different isomeric states of a nucleus can be used to modify the initial isomeric composition [32]. We propose to use a similar method, but using gamma rays with small bandwidth directed onto the stable target nuclei. Compared to Coulomb excitation or Bremsstrahlung spectra, the excitation is far more selective and a much higher conversion rate can be achieved due to the high gamma ray flux density.

Moreover, photoexcitation with small bandwidth γ rays allows moreover the selective excitation of individual levels or groups of levels that decay preferentially to the nuclear isomer, thus enhancing the specific activity of the isomer. Only in few cases the energies of such (groups of) levels are already known. Note that relatively low gamma ray energies may be sufficient for such a pumping to isomeric states. In ^{125}Te a $7/2^+$ state at only 402 keV excitation energy can serve as gateway state for pumping from the $1/2^+$ ground state to the $11/2^-$ isomer at 145 keV [33].

We will estimate the achievable specific activity at the example of ^{115}In for which the required transition energies, branching ratios and transition strengths are already experimentally known, even if this isomer has presently no application in nuclear medicine. The $9/2^+$ ground state of ^{115}In can be excited by an $E2$ transition from the ground state to the $5/2^+$ level at 1078.2 keV that decays with 16% cumulative branching ratio to the $1/2^-$ isomer at 336 keV [33]. The gateway level

at 1078 keV has a half-life of 0.99 ps, corresponding to a total width Γ of 0.67 meV. The fractional width to the ground state Γ_γ is 0.55 meV, while the decay to the isomer has a width of $\Gamma_d = 0.10$ meV. Hence, with the formula of equation 6 we obtain at the resonance energy $E_r = 1078$ keV a peak cross-section of $\sigma(1078 \text{ keV}) = 3400$ b. The product of peak cross-section times width is 2.3 eV·b. With a γ beam flux density per eV of $10^{16} \gamma/(\text{cm}^2 \cdot \text{s} \cdot \text{eV})$ we obtain ^{193m}Ir with a specific activity of 20 GBq/mg at saturation, i.e. $R_\gamma = 10^{-4}$.

In many nuclei only a small fraction of excited levels and transitions between them are experimentally known, in particular for higher excitation energies. Also present theoretical models do not allow to predict the exact position and decay modes of higher-excited levels. Only in particular cases the population of high-spin isomers can be explained with individual intermediate levels from experiment and theory, see e.g. [27,30,34].

Experimental data on isomer population by (γ, γ') reactions had so far been obtained with Bremsstrahlung spectra of large bandwidth. The integrated cross-sections at γ energies of 4 and 6 MeV, respectively, are of the order of 10 to 100 b·eV.

Many potential gateway states that could serve for pumping nuclei from their ground state to isomeric levels are expected to exist, but they still need to be identified by dedicated high resolution measurements from excitation energies of few hundred keV up to close to the particle separation energy. These measurements have to be performed with the new γ beams for each of the isotope for several thousand energy windows, in order to determine the best excitation deexcitation path to the isomer. Presently existing γ -ray beam facilities do not provide sufficiently monochromatic γ -ray beams to search for suitable resonance regions. A systematic investigation will require Compton backscattering facilities such as MEGA-Ray or ELI-NP.

Selecting γ ray energies providing strong pumping to the isomeric state will improve the achievable specific activity correspondingly. Even multiple excitations of the path to the isomer are possible. Due to the missing energy match, no significant back-pumping from the isomer to the ground state will occur.

Note that for populating isomeric levels in (γ, γ') reactions they do not necessarily need to be excited close to the neutron binding energy. To prevent competing photonuclear reactions, it is actually more favorable to select the lowest excited levels that decay populate with sufficiently high yield the isomeric level.

Two examples of long-lived isomers with important medical applications are discussed in the following:

1. ^{195m}Pt :

Platinum compounds such as cisplatin or carboplatin are known to be cytotoxic and are frequently used for chemotherapy of tumors. Labeling these com-

pounds with platinum radiotracers allows for in-vivo pharmacokinetic studies and tumor imaging, e.g. to monitor the patient-specific uptake and optimize the dosing individually [35]. Failure to demonstrate the tumor uptake of the chemotherapy agent by nuclear imaging helps to exclude those “non-responding” patients from unnecessary chemotherapy treatment. ^{195m}Pt has 4 days half-life and emits a 99 keV gamma ray that can be used for imaging by SPECT or gamma cameras. ^{195m}Pt emits also low-energy conversion and Auger electrons. Hence, when used in higher activities, it could be suitable for a combined chemo- and radionuclide therapy. Unfortunately ^{195m}Pt is destroyed by (n, γ) reactions with a very high cross section of 13000 barn. Therefore the specific activity achievable by neutron capture on ^{194}Pt is seriously limited. Even at the HFIR reactor in Oak Ridge only 0.04 GBq/mg are obtained [26] and too little activity is presently available for clinical trials [36]. By (γ, γ') reactions we expect to obtain much higher specific activities, namely about 70 GBq/mg! About 20 GBq could be produced per day, sufficient for several hundred patient-specific uptake measurements or to launch first clinical trials for radionuclide therapy with ^{195m}Pt . Moreover, even if natural platinum or platinum compounds are irradiated, the radionuclidic purity of the product will be excellent since no other long-lived radioisotopes can be produced by activation with few MeV gamma rays.

2. ^{117m}Sn :

Also ^{117m}Sn emits low-energy conversion and Auger electrons, making it promising for radionuclide therapy. In addition it emits a 159 keV gamma ray for imaging. It has been shown that ^{117m}Sn can be used for pain palliation in bone metastases of various cancers. Due to its soft electron energy spectrum it has less side effects on the bone marrow than other radioisotopes with more penetrating radiation [37]. Unfortunately the high-spin isomer ^{117m}Sn is poorly produced in thermal neutron capture on zero-spin ^{116}Sn . With inelastic neutron scattering $^{117}\text{Sn}(n_{\text{fast}}, n' \gamma)$ specific activities of 0.2 to 0.4 GBq/mg are obtained at high flux reactors [26,38], but too little activity is presently available [36]. Production via (γ, γ') reactions with 6 MeV γ beams allows boosting the specific activity at least to 7 GBq/mg. About 0.6 GBq ^{117m}Sn are produced per day, sufficient to start clinical trials.

These two isomers appear at present most interesting for nuclear medicine applications. The specific activity and total production per day could be significantly improved with still to be found better gateway states. A detailed search for suitable gateway states at an upcoming γ -beam facility with small bandwidth is urgently needed.

Table 3 Estimated production rates of radioisotopes produced in (γ, n) , (γ, p) or $(\gamma, 2n)$ reactions. Experimental cross sections were taken from [19], estimated cross sections are marked in italics. The fraction of the maximum specific activity produced in (γ, x) reactions R_γ , is put in relation to that obtained with (n, γ) reactions $R_{(n, \gamma)}$ at a thermal neutron flux of 10^{14} n/(cm² s) in the last column. *: For comparison we show the values for ^{99}Mo produced by $^{98}\text{Mo}(n, \gamma)$. However, usually ^{99}Mo is produced by fission with much better specific activity.

Product isotope	$T_{1/2}$ d	Target isotope	Reaction	E_γ MeV	σ b	Spec. act. γ beam GBq/mg	Activity per day GBq	R_γ fraction of max.	Spec. act. high flux reactor GBq/mg	$R_\gamma/R_{(n, \gamma)}$
^{47}Ca	4.5	^{48}Ca	(γ, n)	19	0.09	1100	400	0.05	0.9	1200
^{64}Cu	0.5	^{65}Cu	(γ, n)	17	0.09	830	1150	0.006	4	200
^{99}Mo	2.8	^{100}Mo	(γ, n)	14	0.16	960	350	0.06	0.08*	12000
^{103}Pd	17	^{104}Pd	(γ, n)	17	<i>0.05</i>	290	16	0.1	1.8	160
^{165}Er	0.4	^{166}Er	(γ, n)	13	0.3	1100	1100	0.016	4.7	230
^{169}Er	6.9	^{170}Er	(γ, n)	12	<i>0.3</i>	≈ 800	130	≈ 0.2	0.8	1000
^{186}Re	3.7	^{187}Re	(γ, n)	15	0.6	≈ 1400	320	≈ 0.2	35	40
^{225}Ra	14.8	^{226}Ra	(γ, n)	12	<i>0.2</i>	≈ 300	30	≈ 0.2		
^{47}Sc	3.4	^{48}Ti	(γ, p)	19	<i>0.02</i>	250	100	0.009		
^{67}Cu	2.6	^{68}Zn	(γ, p)	19	<i>0.03</i>	260	115	0.01		
^{44}Ti	60 y	^{46}Ti	$(\gamma, 2n)$	27	<i>0.01</i>	≈ 0.5	0.008	≈ 0.1		
^{224}Ra	3.7	^{226}Ra	$(\gamma, 2n)$	16	<i>0.1</i>	≈ 50	10	≈ 0.01		

6.2 Radioisotopes via the (γ, n) reaction

When being excited well beyond the neutron binding energy a nucleus loses readily a neutron. Competing reactions such as deexcitation by gamma ray emission are far less probable.

1. $^{99}\text{Mo}/^{99m}\text{Tc}$:

The presently most used radioisotope for nuclear medicine studies is ^{99m}Tc . Its 140 keV γ ray is ideal for SPECT imaging. With a relatively short half-life of 6 h and the quasi-absence of beta particles the radiation dose to the patient is low. ^{99m}Tc is conveniently eluted in non-carrier-added quality from simple and reliable ^{99}Mo ($T_{1/2} = 66$ h) generators that can be used for about one week. Various technetium compounds have been developed for a multitude of nuclear medicine applications [1]. The combination of these advantages explains why ^{99m}Tc is used in about 80% of all nuclear medicine studies. 28 millions applications employing ^{99m}Tc are performed per year. Every week more than 80 kCi (3000 TBq) of ^{99}Mo have to be produced to load the $^{99}\text{Mo}/^{99m}\text{Tc}$ generators that are shipped to the ^{99m}Tc users (mainly hospitals) or to radiopharmacies. Until recently five nuclear reactors were used to produce about 95% of the world needs of ^{99}Mo by neutron-induced fission of highly enriched ^{235}U targets. Recently the two reactors that used to produce the majority of the ^{99}Mo supply had extended shutdowns, leading to a serious $^{99}\text{Mo}/^{99m}\text{Tc}$ supply crisis [39, 40]. This triggered large interest in alternative $^{99}\text{Mo}/^{99m}\text{Tc}$ production paths. One alternative production path uses the $^{100}\text{Mo}(\gamma, n)$ reaction. Usual Bremsstrahlung facilities produce ^{99}Mo with limited specific activity that

makes it more difficult to use the established generator technology (acid alumina columns). With γ beams of high flux density, ^{99}Mo could be produced with much higher specific activity, allowing direct use of existing generator technology. A facility providing $10^{15}\gamma/\text{s}$ could produce via $^{100}\text{Mo}(\gamma, n)$ reactions several TBq per week. Thus, many such facilities would be required to assure the worldwide ^{99}Mo supply.

This example demonstrates that the new production method by γ beams is not intended to compete with large-scale production of established isotopes. The advantage of γ beams for radioisotope production lies clearly in the very high specific activity that can be achieved for radioisotopes or isomers that are very promising for nuclear medicine, but that are presently not available in the required quality or quantity. Examples of such isotopes and new clinical applications that may become available with such radioisotopes produced by γ beams will be discussed in the following.

2. $^{225}\text{Ra}/^{225}\text{Ac}$:

Alpha emitters are very promising for therapeutic applications, since the emitted alphas deposit their energy very locally (typical range of one to few cancer cell diameters) with high linear energy transfer (LET) and, hence, high probability for irreparable double strand breaks. An alpha emitter coupled to a cancer cell specific bioconjugate can be used for targeted alpha therapy to treat disseminated cancer types (leukemia), micro-metastases of various cancers or to destroy chemo- and radiation-resistant cancer cells (e.g. glioblastoma). One promising alpha emitter is ^{225}Ac ($T_{1/2} = 10$ days) that decays by a series of four alpha decays and two beta de-

Table 4 Radioisotopes of the neptunium chain produced in the $^{226}\text{Ra}(\gamma, n)^{225}\text{Ra}$ reaction and subsequent decays.

Isotope	α energy (MeV)	Mean β energy (MeV)	$T_{1/2}$
^{225}Ra		0.1	15 d
^{225}Ac	5.8		10 d
^{221}Fr	6.3		4.9 min
^{217}At	7.1		32 ms
^{213}Bi	5.8 (2%)	0.4 (98%)	46 min
^{213}Po	8.4		4.2 μs
^{209}Pb		0.2	3.25 h

cays to ^{209}Bi , see table 4. ^{225}Ac (valence III) can either be used directly for targeted alpha therapy, or as generator for ^{213}Bi that is used for targeted alpha therapy. Today ^{225}Ac is produced by decay of $^{229}\text{Th} \rightarrow ^{225}\text{Ra} \rightarrow ^{225}\text{Ac}$ and chemical separation. Unfortunately only small quantities (about 1 Ci=37 GBq per year) are available [41], which is far too little for a large scale application. Alternatively, ^{226}Ra can be converted by (p,2n) reactions to ^{225}Ac [42] or by (γ, n) reactions to ^{225}Ra that decays to ^{225}Ac and is subsequently chemically separated from the ^{226}Ra target [43]. The radioactive ^{226}Ra targets are difficult to handle, when the activity of the target gets important. Therefore a γ beam with high flux density is essential to minimize the target size and target activity while maximizing the product activity. Thus about 200 GBq ^{225}Ac could be produced per week, enough to treat hundreds of patients.

3. ^{169}Er :

^{169}Er decays with 9.4 days half-life by low-energy beta emission (100 keV average beta energy). These betas have a range of 100 to 200 μm in biological tissue, corresponding to few cell diameters. The short beta range makes this isotope very interesting for targeted radiotherapy [44]. However, due to the low $^{168}\text{Er}(n_{\text{th}}, \gamma)$ cross section it cannot be produced with high specific activity³ by neutron capture. Using intense γ beams one can reach significantly higher specific activities via $^{170}\text{Er}(\gamma, n)$ reactions.

4. ^{165}Er :

^{165}Er is one example for an isotope that decays mainly by low-energy Auger electrons. Their range is shorter than one cell diameter. Hence, these Auger emitters have to enter the cell and approach the cell's nucleus to damage the DNA and destroy a cell. Coupled to a bioconjugate that is selectively internalized into cancer cells it can enhance the ratio for dose equivalent delivered to the tumor cell with respect to normal cells. This should result in an improved

tumor treatment with less side effects. R&D to identify suitable bioconjugates is under way [46].

5. ^{47}Sc :

^{47}Sc is a promising low-energy beta emitter for targeted radiotherapy. Scandium is the lightest rare earth element. Most established labeling procedures for valence III metals (Y, Lu, ...) can be applied directly for Sc. Its 159 keV gamma line allows imaging of ^{47}Sc distribution by SPECT or gamma cameras. Alternatively the β^+ emitting scandium isotope ^{44}Sc can be used for PET imaging as a "matched pair". Carrier-free ^{47}Sc can be produced by $^{50}\text{Ti}(p, \alpha)$ or $^{47}\text{Ti}(n_{\text{fast}}, p)$ reactions followed by chemical separation. The alternative production via $^{46}\text{Ca}(n, \gamma)^{47}\text{Ca} \rightarrow ^{47}\text{Sc}$ is uneconomic due to the extremely low natural abundance of ^{46}Ca . At present too little ^{47}Sc is available [36], but with intense γ beams the production via $^{48}\text{Ca}(\gamma, n)^{47}\text{Ca} \rightarrow ^{47}\text{Sc}$ becomes competitive. After grow-in of ^{47}Sc it is chemically separated from the irradiated calcium, which, after sufficient decay of ^{47}Ca , can be reused to form a new irradiation target.

6. ^{64}Cu :

^{64}Cu is a relatively long-lived β^+ emitter ($T_{1/2} = 12.7$ h) with various applications in nuclear medicine [47]. ^{64}Cu -ATSM is a way to measure hypoxia of tumors. Hypoxia is an important effect influencing the resistance of tumor cells against chemo- or radiation therapy. ^{64}Cu can also act itself as therapeutic isotope due to its emission of β^- (191 keV mean energy) and low energy Auger electrons. Today ^{64}Cu is mainly produced with small cyclotrons by the $^{64}\text{Ni}(p, n)$ reactions. Alternative production by $^{65}\text{Cu}(\gamma, n)$ does not require the rare and expensive ^{64}Ni targets and saves the chemical separation step.

7. ^{186}Re :

^{186}Re is a radioisotope suitable for bone pain palliation, radiosynovectomy and targeted radionuclide therapy. Rhenium is chemically very similar to its homologue technetium, thus known compounds that have been developed for imaging with ^{99m}Tc can also be labeled with ^{186}Re and used for therapy. ^{186}Re is currently either produced by neutron capture on ^{185}Re , resulting in limited specific activity, or by $^{186}\text{W}(p, n)$ reactions followed by chemical Re/W separation. The latter guarantees excellent specific activity at the expense of much reduced production rates and a required chemical separation. Production by $^{187}\text{Re}(\gamma, n)$ would allow producing larger amounts (2 TBq per week) of ^{186}Re with high specific activity. Enriched ^{187}Re targets should be used to minimize contamination of the product with long-lived $^{184,184m}\text{Re}$ by $^{185}\text{Re}(\gamma, n)$ reactions.

8. "Slightly neutron-deficient radioisotopes":

"Slightly neutron-deficient isotopes" are decaying by electron capture with emission of X-rays and low-energy Auger electrons, partially also gamma rays

³ Today ^{169}Er with low specific activity is actually used for radiation synovectomy to treat inflamed small joints, e.g. in fingers [45].

and conversion electrons. The absence of beta emission and the presence of low-energy X-rays or electrons is of advantage for a variety of applications such as calibration sources, radionuclide therapy applications after internalization into cells, etc. All these isotopes can be produced by neutron capture on the stable ($A-1$) neighboring isotope. However, as shown in Tab. 5, the latter is generally very rare in nature (since only produced by unusual astrophysical processes like the p-process) and correspondingly costly when produced as isotopically enriched target material. Using instead (γ, n) reactions to populate the same isotopes allows using the much more abundant, and hence cheaper, ($A+1$) neighboring isotope as target. An example is ^{103}Pd , a low-energy electron emitter. It can be used for targeted radionuclide therapy (coupled to a suitable bioconjugate) or for brachytherapy applications, where sources (“seeds”) are inserted into a cancer (e.g. breast cancer [48, 49]) for localized irradiation. However, the target ^{102}Pd for production by neutron capture is rare and expensive. Production via $^{104}\text{Pd}(\gamma, n)$ is more economic, if sufficiently intense γ beams become available. The same applies to other radioisotopes or isomers shown in table 5 that have applications in nuclear medicine or other fields.

6.3 Radioisotopes via the (γ, p) reaction

Even when excited beyond the proton binding energy, a nucleus does not necessarily lose a proton. The latter is bound by the Coulomb barrier, leading to a suppression of the proton loss channel. Only for excitation well beyond the proton binding energy, the proton gains enough kinetic energy for tunneling efficiently through the Coulomb barrier. However, such excitation energies are usually also above the neutron binding energy or even the two-neutron binding energy. Hence neutron emission competes with proton emission and the cross sections for (γ, p) reactions may be one order of magnitude lower than the competing channels (compare Fig. 3). Thus, the achievable specific activity (specific activity with respect to the target mass) is limited for (γ, p) reactions. However, the product isotope differs chemically from the target since it has one proton less ($Z_{\text{product}} = Z_{\text{target}} - 1$). After irradiation a chemical separation of the product isotope from the target can be performed, ultimately resulting in a high specific activity that is only compromised by competing reactions leading to other isotopes of the product element (such as (γ, np) , $(\gamma, 2n)EC/\beta^+$, etc.) or product burn-up by (γ, n) .

1. ^{47}Sc :

Besides the $^{48}\text{Ca}(\gamma, n)^{47}\text{Ca} \rightarrow ^{47}\text{Sc}$ reaction, ^{47}Sc can also be produced via the $^{48}\text{Ti}(\gamma, p)^{47}\text{Sc}$ reaction. The established Sc/Ti separation schemes can be

Table 5 Comparison of target isotopes required for (n, γ) and (γ, n) reactions respectively leading to the same radioisotopes or isomers. These have applications in nuclear medicine or other fields. The last column shows the ratio of the natural abundances of the $A+1$ and $A-1$ targets.

Product isotope	$T_{1/2}$ (d)	(n, γ) target	nat. abun. (%)	(γ, n) target	nat. abun. (%)	$[A+1]$ / $[A-1]$
^{47}Ca	4.5	^{46}Ca	0.004	^{48}Ca	0.187	47
^{51}Cr	27.7	^{50}Cr	4.3	^{52}Cr	84	20
^{55}Fe	996	^{54}Fe	5.8	^{56}Fe	92	16
^{75}Se	120	^{74}Se	0.89	^{76}Se	9.4	11
^{85}Sr	65	^{84}Sr	0.56	^{86}Sr	9.9	18
^{97}Ru	2.9	^{96}Ru	5.5	^{98}Ru	1.9	0.3
^{103}Pd	17	^{102}Pd	1.0	^{104}Pd	11.1	11
^{109}Cd	463	^{108}Cd	0.89	^{110}Cd	12.5	14
^{113}Sn	115	^{112}Sn	0.97	^{114}Sn	0.66	0.7
^{121}Te	16.8	^{120}Te	0.09	^{122}Te	2.6	29
^{127}Xe	36	^{126}Xe	0.09	^{128}Xe	1.9	21
^{133m}Ba	1.6	^{132}Ba	0.1	^{134}Ba	2.4	24
^{139}Ce	138	^{138}Ce	0.25	^{140}Ce	88	352
^{153}Gd	239	^{152}Gd	0.2	^{154}Gd	2.2	11
^{159}Dy	144	^{158}Dy	0.095	^{160}Dy	2.3	24
^{165}Er	0.43	^{164}Er	1.6	^{166}Er	33.5	21
^{169}Yb	32	^{168}Yb	0.13	^{170}Yb	3.04	23
^{175}Hf	70	^{174}Hf	0.16	^{176}Hf	5.3	33
^{181}W	121	^{180}W	0.12	^{182}W	26.5	221
^{191}Pt	2.8	^{190}Pt	0.014	^{192}Pt	0.78	56
^{193m}Pt	4.3	^{192}Pt	0.78	^{194}Pt	33	42

employed for the chemical processing. Compared to the $^{47}\text{Ti}(n, p)$ way here the direct production of disturbing long-lived ^{46}Sc (via $^{46}\text{Ti}(n, p)$ or $^{47}\text{Ti}(\gamma, p)$, respectively) can be limited more easily, since ^{48}Ti is the most abundant titanium isotope and can be enriched more easily to high abundance. However, the irradiation times have to be kept relatively short to prevent excessive formation of ^{46}Sc impurity by $^{47}\text{Sc}(\gamma, n)$ reactions.

2. ^{67}Cu :

^{67}Cu is also a promising beta-emitter for targeted radiotherapy. Alike ^{47}Sc it has a sufficiently long half-life for accumulation in the tumor cells when bound to antibodies and its 185 keV gamma ray allows imaging with SPECT or gamma cameras. Together with the PET imaging isotopes ^{61}Cu or ^{64}Cu it forms a “matched pair”. The usual production routes $^{68}\text{Zn}(p, 2p)$, $^{70}\text{Zn}(p, \alpha)$ or $^{64}\text{Ni}(\alpha, p)$ are all characterized by low yields. The former requires energetic protons ($\gg 30$ MeV from larger cyclotrons) and the latter two methods use expensive enriched targets with low natural abundances. The alternative production via $^{67}\text{Zn}(n, p)$ requires a very high flux of fast neutrons, which is only available in few reactors. At present clinical trials with ^{67}Cu are

Table 6 Therapy radioisotopes that can be produced in (γ, p) reactions

isotope	mean beta energy (keV)	$T_{1/2}$ (days)	target isotope natural abundance (%)
^{47}Sc	162	3.35	^{48}Ti (73.7%)
^{67}Cu	141	2.58	^{68}Zn (18.7%)
^{131}I	182	8.03	^{132}Xe (26.9%)
^{161}Tb	154	6.91	^{162}Dy (25.5%)
^{177}Lu	134	6.65	^{178}Hf (27.3%)

hindered by insufficient supply [36]. Production via $^{68}\text{Zn}(\gamma, p)$ reactions induced by intense γ beams provides higher activities and uses more abundant, and, hence cheaper ^{68}Zn targets. The established Cu/Zn separation schemes can be employed for the required chemical processing.

3. Isotopes with higher Z :

In principle also heavier β^- emitters used for radionuclide therapy such as ^{131}I , ^{161}Tb or ^{177}Lu could be produced by (γ, p) reactions (on ^{132}Xe , ^{162}Dy or ^{178}Hf targets respectively). However, for higher Z the increasing Coulomb barrier leads to small production cross sections. Production in high flux reactors by neutron-induced fission (for ^{131}I) or by neutron capture on the $(A - 1, Z - 1)$ target (^{130}Te , ^{160}Gd or ^{176}Yb respectively), followed by decay and chemical separation leads to products with excellent specific activity and is more economic.

6.4 Radioisotopes via the ($\gamma, 2n$) reaction

1. ^{44}Sc :

^{44}Sc is a promising metallic PET tracer that emits a 1157 keV gamma-ray quasi-simultaneously with the positron. With a suitable detection system (Compton telescope plus PET camera), a triple coincidence (gamma rays of 511 keV, 511 keV, and 1157 keV) can be detected [50]. Hence, for each triple-event the point of emission is derived instead of the usual line-of-response, leading to improved position resolution at reduced dose to the patient. Moreover ^{44}Sc forms a “matched pair” with ^{47}Sc , a therapy isotope discussed above. ^{44}Sc can be obtained from $^{44}\text{Ti}/^{44}\text{Sc}$ generators where the parent isotope ^{44}Ti is very long-lived ($T_{1/2} = 60$ years). Despite the very favorable properties of ^{44}Sc , this isotope is not yet used in clinical routine, since the generator isotope ^{44}Ti is difficult to produce and therefore prohibitively expensive. The current cost for 200 MBq of ^{44}Ti , the typical activity for one $^{44}\text{Ti}/^{44}\text{Sc}$ generator for human use, is about 2 million EUR! Exposing enriched ^{46}Ti (natural abundance 8%) to an intense γ beam allows

producing ^{44}Ti by ($\gamma, 2n$) reactions. It will take about three weeks of irradiation in a mid-sized γ beam facility to generate 200 MBq of ^{44}Ti , but such a generator (or several subsequent generators that use the same recycled ^{44}Ti activity) can be eluted several times a day and serve for tens of years.

2. $^{224}\text{Ra}/^{212}\text{Pb}/^{212}\text{Bi}$:

Via $^{226}\text{Ra}(\gamma, 2n)$ reactions the isotope ^{224}Ra ($T_{1/2} = 3.66$ d) from the thorium chain can be obtained, where the noble gas ^{220}Rn isotope can be extracted easily. The α emitter ^{212}Bi ($T_{1/2} = 60$ min) in this decay chain or its mother isotope ^{212}Pb are also considered for targeted alpha therapy, e.g. for malignant melanoma metastases [51, 52].

6.5 Other photonuclear reaction channels

In ($\gamma, 2p$) reactions even two protons must overcome the Coulomb barrier, making this reaction channel even less likely than the (γ, p) reaction. Measured cross-sections for ($\gamma, 2p$) reactions exist for $^{63}\text{Cu}(\gamma, 2p)^{61}\text{Co}$ [53]. They range from few μ -barn at 30 MeV to 14 μ barn at 60 MeV. Also for (γ, α) reactions the higher Coulomb barrier leads to small cross-sections in the microbarn range. Usually other production reactions provide better yields, making these types of photonuclear reaction less competitive.

Photo-fission of uranium or thorium targets allows production of ^{99}Mo and other isotopes with highest specific activity. However, the here proposed γ beams with high flux density are not suitable since they lead to an excessive target heating. In each fission about 200 MeV are released, the dominant part as kinetic energy of the fission fragments that will stop within few μm range. This would lead to power densities of several hundred kW per cm^3 , impossible to cool from the targets.

7 Photonuclear Activation for Brachytherapy Applications

Certain nuclear medicine applications use the radioisotopes “directly”, i.e. not necessarily coupled to a biomolecule.

There are various applications for micro- or nanoparticles that are doped with radioisotopes. They can be used for radioembolization of, e.g., liver cancer or liver metastases [54]. The radioactive microparticles are directly injected into the arteries supplying the tumor, then irradiate the latter with their medium-range radiation (beta particles, low-energy X-rays or gamma rays). Similarly, nanoparticles are considered for targeting tumors. The radioisotopes can be introduced into the micro- or nanoparticles in various ways:

1. The radioisotopes can be added to the raw materials used in the chemical synthesis of the micro- or nanoparticles. However, this makes the processing much more involved, since radioactive material

has to be handled and the respective radiological and contamination issues have to be addressed in the production facility.

2. The radioisotopes can be implanted in form of a radioactive ion beam into the ready-made micro- or nanoparticles [55]. This method is quite universal, allowing to dope even with radioisotopes of elements that are usually not soluble in or chemically compatible with the matrix. However, the radioactive isotopes first need to be brought into a radioactive ion beam which may be more involved depending on the chemical element.
3. A stable precursor of the radioisotope can be introduced prior to the chemical synthesis of the micro- or nanoparticles or ion-implanted after synthesis. Then the precursor is transmuted in a nuclear reaction into the desired radioisotope. However, the micro- or nanoparticles may be sensitive to radiation damage. Hence activation ,e.g., in a nuclear reactor could damage them such that they are no longer usable in in-vivo applications. For neutron activation it has been shown that resonance capture of epithermal neutrons (“adiabatic resonance crossing” method) can be of advantage to overcome this problem [56]. Here we propose a complementary method of activation by photonuclear reactions. For the isotopes listed in table 5 the general advantages discussed above apply. In addition the high cross section ratio of “useful” photonuclear reactions versus “disturbing” reactions causing radiation damage allows obtaining relatively high activities.

Radioisotopes can also be bound in larger solid matrices that are then mechanically (surgically) introduced into the body or brought close to it to irradiate tumors or benign diseases. Such a so-called brachytherapy is today routinely used to treat prostate cancer by permanently introduced seeds containing radioactive ^{125}I [57]. It is also useful to prevent in-stent restenosis by intravascular brachytherapy using radioactive stents [58], prevent closure of the pressure relief channel in glaucoma filtering surgery by radioactive implants [59] or perform other anti-inflammatory or anti-proliferative treatments. Photonuclear reactions could simplify the production of the respective stents or seeds. Instead of introducing the radioactive isotopes in the production process or ion-implanting it afterwards, it will be possible to produce the stents or seeds in their final form and then activate a previously included stable precursor isotope by photonuclear reactions. Selective photonuclear reactions assure to keep the radiation damage of the matrix low and avoid an unwanted production of disturbing radioisotopes by activation of the matrix.

8 Advantages of the Proposed Photonuclear Reactions over Existing Technologies

The intense brilliant γ beam will allow to produce radioisotopes with rather high specific activity. Advantages of γ ray beams with small opening angle are:

- The produced radioisotopes are concentrated in a small target volume, hence resulting in much higher specific activity than usual.
- Much less of the (often costly) target material is required.
- Radioactive targets are more efficiently converted into the required product isotopes, hence more compact and less active targets can be employed, resulting in less activity to be handled and less dose rate.

Additional advantages when using the low bandwidth γ ray beams are:

- The higher cross section for monochromatic beams leads to a short interaction length (cm or less). This leads to an additional reduction of the required target mass, hence further reducing the target costs and increasing the specific activity.
- Compared to Bremsstrahlung beams a much reduced γ ray heating per useful reaction rate occurs since the γ rays in the useful energy range are not accompanied by an intense low-energy tail. Moreover the usual equilibrium between γ -rays and electrons (which are responsible for the actual heating) will build up only for very thick targets.
- Much reduced radiation damage due to quasi-monochromatic beams will make it possible to first dope and then activate materials (e.g. organic, nanoscale,...) that would not withstand irradiation in a nuclear reactor or a bremsstrahlung γ ray spectrum.
- Isotopic enrichment may not necessarily be needed, when for a given γ energy the wanted cross section is much higher than for other isotopes. In particular, the fine structure of the Pygmy dipole resonance (PDR), probably similar to the giant dipole resonance (GDR), could be exploited.
- Also less stringent requirements exist concerning isotopic enrichment or chemical impurities of the target materials if the γ ray energy is chosen such that the maximum cross sections of the wanted production channels corresponds to minima in the cross section of activation of impurities.
- Selective production reduces the overall activity level of the irradiated target and reduces the challenge to the chemical post-processing.

Moreover, there are practical advantages of photonuclear reactions compared to charged-particle induced reactions: Radioactive targets like ^{226}Ra or targets that risk to react heavily in contact with cooling water (e.g. alkali metals) can be safely encapsulated into relatively

thick metal walls, since gamma rays penetrate easily and cause less heating of the walls than charged particles do.

A further optional increase of the specific activity is possible by:

- Enriched target isotopes may be used.
- A thin target or a stack of thin target foils interleaved with a different solid, liquid or gas that acts as catcher of recoil ions. Extraction and separation of the recoiled product isotopes can be performed with the usual radiochemical methods.
- If the produced radioisotope belongs to a different chemical element than the target (e.g. for (γ, p) reactions), a usual radiochemical post-processing (e.g. ion exchange chromatography, liquid-liquid extraction, etc.) can be employed to separate the product element from remainders of the target element and thus increase the specific activity of the product.
- A product isotope that decays to a radioactive daughter isotope with medical applications allows producing a generator.

Conclusion and Outlook

Laser beams revolutionized atomic physics and its applications, not only due to their coherence, but often just due to their high photon flux density or their high spectral photon flux density. Similarly gamma beams open many new possibilities in nuclear physics and its applications. Alike in atomic physics such beams can be used to pump a good fraction of the nuclear ground state population via excited levels into an isomeric state. While (far) ultraviolet laser beams can efficiently photoionize atoms by exciting a valence electron to an unbound state, energetic gamma beams can efficiently excite a nucleon (neutron or proton) into an unbound state leading to photodissociation and creation of a new isotope. When these reactions are resonantly enhanced the monochromaticity of laser or gamma beams respectively is decisive.

Using the new γ beam facilities we can use compact targets, which are exposed to the gamma radiation and undergo photonuclear reactions such as (γ, γ') , (γ, n) , (γ, p) , etc. to form radioisotopes. After a suitable irradiation time, a radioisotope with high specific activity is produced. After the usual radiochemical and radiopharmaceutical steps (such as optionally dissolving of the target, optionally chemical purification, labeling, quality control, ...) a radiopharmaceutical product is created for use in diagnostic or therapeutic nuclear medicine procedures. The produced radioisotope may be used directly for nuclear medicine applications.

The investment and running costs of the proposed γ beam facilities are of the order of 40 MEUR and few MEUR/year. This is cheaper than a high-flux reactor, but more expensive than compact cyclotrons that provide charged particle beams with 10 to 20 MeV energy suitable for production of PET tracers. World-wide more

than 600 such cyclotrons exist, often based at hospitals or close-by. They provide regularly the short-lived PET isotopes ^{18}F ($T_{1/2} = 110$ min), ^{11}C (20 min), ^{13}N (10 min) and ^{15}O (2 min) for molecular imaging applications. Although it would be possible to produce also such isotopes by photonuclear reactions (e.g. $^{20}\text{Ne}(\gamma, np)^{18}\text{F}$), a more complex Compton backscattering facility would be clearly an overkill for such applications.

The selection of radioisotopes presently used in nuclear medicine routine applications is actually dictated by the radioisotope's availability at reasonable costs. This selection is not necessarily optimized for all clinical applications with respect to optimum nuclear (half-life, decay radiation) and chemical properties (labeling efficiency, in-vivo stability of compounds, etc.). Other radioisotopes might be advantageous for the patient but are presently not available. The main advantage of the γ beam facility is the new and rather unique access to radioisotopes or isomers with high specific activity that can complement and extend the choice of radioisotopes for nuclear medicine applications.

Acknowledgement

We acknowledge helpful discussions with C. Barty and R. Hajima. We enjoyed the close collaboration with V. Zamfir, who is heading ELI-NP. We were supported by the DFG Clusters of Excellence: Munich Centre for Advanced Photonics (MAP) and UNIVERSE.

References

1. Ch. Schiepers, *Diagnostic Nuclear Medicine*, Springer Verlag, Berlin (2006).
2. G.J.R. Cook, *Clinical Nuclear Medicine*, Hodder Arnold Publisher, London (2006).
3. J.C. Reubi, H.R. Mäcke, E.P. Krenning, *Candidates for Peptide Receptor Radiotherapy Today and in the Future*, J. Nuc. Med. **46**, 67S (2005).
4. C.A. Boswell and M.W. Brechbiel, *Development of radioimmunotherapeutic and diagnostic antibodies: an inside-out view*, Nucl. Med. Biology **34**, 757 (2007).
5. G.J. Beyer, *Radioactive ion beams for biomedical research and nuclear medical applications*, Hyp. Interactions **129**, 529 (2000).
6. J.C. Reubi, J.-C. Schär, B. Wasser, S. Wenger, A. Heppler, J.S. Schmidt, H.R. Mäcke, *Affinity profiles for human somatostatin receptor subtypes SST1-SST5 of somatostatin radiotracers selected for scintigraphic and radiotherapeutic use*, Eur. J. Nucl. Med. **27**, 273 (2000).
7. H.R. Maecke, M. Hofmann and U. Haberkorn, *(68)Ga-labeled peptides in tumor imaging*, J. Nucl. Med. **46** Suppl 1, 172S (2005).
8. U. Kneissl, N. Pietralla, A. Zilges, *Low-lying dipole modes in vibrational nuclei studied by photon scattering*, J. Phys. G **32**, R217 (2006).
9. H.R. Weller, M.W. Ahmed, H. Gao, W. Torrow, U.K. Wu, M. Gai, R. Miskimen, *Research opportunities*

- at the upgraded HI γ S facility, Prog. Part. Nucl. Phys. **62**, 257 (2009).
10. W.J. Brown, S.G. Anderson, C.P.J. Barty, S.M. Betts, R. Booth, J.K. Crane, D.N. Fiffinghoff, D.J. Gibson, F.V. Hartmann, E.P. Hartouni, J. Kuba, G.P. Le Sage, D.R. Slaughter, A.M. Tremaine, A.J. Wootton, P.T. Springer, *Experimental characterization of an ultrafast Thompson scattering x-ray source with three-dimensional time and frequency-domain analysis*, Phys. Rev. ST AB **7**, 060702 (2004).
 11. F. Albert, S.G. Anderson, G.A. Anderson, S.M. Betts, D.J. Gibson, C.A. Hagemann, J. Hall, M.S. Johnson, M.J. Messerly, X.A. Semenov, M.Y. Shoerdin, A.M. Freimaine, F.V. Hartmann, C.W. Siders, D.P. McNabb, C.P.J. Barty, *Isotope-specific detection of low-density materials with laser-based monoenergetic gamma-rays*, Opt. Lett. **35**, 354 (2010).
 12. C. Barty, *Development of MEGa-Ray technology at LLNL*; [http://www.eli-np.ro/executive committee-meeting-april12-13.php](http://www.eli-np.ro/executive_committee-meeting-april12-13.php) (2010).
 13. <http://www.eli-np.ro/>
 14. R. Hajima, N. Kikuzawa, N. Nishimori, T. Hayakawa, T. Shizuma, K. Kawase, M. Kando, E. Minehara, H. Toyokawa, H. Ohgaki, *Detection of radioactive isotopes by using Compton scattered γ -ray beams*, Nucl. Instr. Meth. **A608**, S57 (2009).
 15. R. Hajima, *High Flux and High Brilliance γ -ray Sources Based on Energy Recovery Linac*; [http://www.eli-np.ro/executive committee-meeting-april12-13.php](http://www.eli-np.ro/executive_committee-meeting-april12-13.php) (2010).
 16. V.N. Litvinenko, I. Ben-Zvi, D. Kayran, I. Pogorelsky, E. Pozdeyev, T. Roser, V. Yakimenko, *Potential Uses of ERL-Based γ -Ray Sources*, IEEE Trans. Plasma Sci. **36**, 1799 (2008).
 17. D. Habs, M. Hegelich, J. Schreiber, M. Gross, A. Henig, D. Kiefer, D. Jung, *Dense laser-driven electron sheets as relativistic mirrors for coherent production of brilliant X-ray and γ -ray beams*, Appl. Phys. **B 93**, 349 (2008).
 18. M.S. Dewey, E.G. Kessler, R.D. Deslattes, H.G. Börner, M. Jentschel, C. Doll, P. Mutti, *Precision measurements of the ^{29}Si , ^{33}S , and ^{36}Cl binding energies*, Phys. Rev. **C73**, 044303 (2006).
 19. <http://www.nndc.bnl.gov/exfor/>
 20. E. Segrè, *Nuclei and Particles*, W.A. Benjamin, Inc. London (1977).
 21. T. von Egidy and D. Bucurescu, *Systematics of nuclear level density parameters*, Phys. Rev. **C 72**, 044311(2005).
 22. H.A. Weidenmüller and G.G. Mitchell, *Random matrices and chaos in nuclear physics: Nuclear structure*, Rev. of Mod. Phys. **81**, 539 (2009).
 23. G.E. Mitchell, A. Richter and H.A. Weidenmüller, *Random Matrices and Chaos in Nuclear Physics: Nuclear Reactions*, Rev. of Mod. Phys. in press (2010).
 24. J.H. Hubbell, H.A. Gimm and I. Øverbø, J. Phys. Chem. Ref. Data **9**, 1023 (1980).
 25. Y.A. Karelin, Y.N. Gordeev, V.T. Filimonov, Y.G. Toporov, A.A. Yadovin, V.I. Karasev, V.M. Lebedev, V.M. Radchenko, R.A. Kuznetsov, *Radionuclide Production at the Russian State Scientific Center, RIAR*, Appl. Radiat. Isot. **48**, 1585 (1997).
 26. F.F.(Russ) Knapp Jr., S. Mirzadeh, A.L.Beeta, M. Du, *Production of therapeutic radioisotopes in the ORNL High Flux Isotope Reactor (HFIR) for applications in nuclear medicine, oncology and interventional cardiology*, J. Radioanal. Nucl. Chem. **263**, 503 (2005).
 27. P. von Neumann-Cosel, A. Richter, C. Spieler, W. Ziegler, J.J. Carroll, T.W. Sinor, D.G. Richmond, K.N. Taylor, C.B. Collins, K. Heyde, *Resonant photoexcitation of isomers, $^{115}\text{In}^m$ as a test case*, Phys. Lett. **B 266**, 9 (1991).
 28. J.J. Carroll, T.W. Sinor, D.G. Richmond, K.N. Taylor, C.B. Collins, M. Huber, N. Huxel, P.v. Neumann-Cosel, A. Richter, C. Spieler, W. Ziegler, *Excitation of $^{123}\text{Te}^m$ and $^{125}\text{Te}^m$ through (γ, γ') reactions*, Phys. Rev. **C 43**, 897 (1991).
 29. J.J. Carroll, M.J. Byrd, D.G. Richmond, T.W. Sinor, K.N. Taylor, W.L. Hodge, Y. Paiss, C.D. Eberhard, J.A. Anderson, C.B. Collins, E.C. Scasbrough, P.P. Antich, F.J. Agee, D. Davis, G.A. Huttlin, K.G. Kerris, M.S. Litz, D.A. Whittaker, *Photoexcitation of nuclear isomers by (γ, γ') reactions*, Phys. Rev. **C 43**, 1238 (1991).
 30. J.J. Carroll, C.B. Collins, K. Heyde, M. Huber, P. von Neumann-Cosel, V.Y. Ponomarev, D.G. Richmond, A. Richter, C. Schlegel, T.W. Sinor, K.N. Taylor, *Intermediate structure in the photoexcitation of $^{77}\text{Se}^m$, $^{79}\text{Br}^m$, and $^{137}\text{Ba}^m$* , Phys. Rev. **C 48**, 2238 (1993).
 31. X. Ledoux, J. Sigaud, T. Granier, J.-P. Lochard, Y. Patin, P. Pras, C. Varignon, J.-B. Laborie, Y. Boulin, F. Gansing, *Measurements of isomeric cross-section ratios for neutron capture in the resonance region*, Eur. Phys. J. **A 27**, 59 (2006).
 32. I. Stefanescu, G. Georgiev, F. Ames, J. Ayströ, D.L. Balabanski, G. Bollen, P.A. Butler, J. Cederkäll, N. Champault, T. Davinson, A. De Maesschalck, P. Delahaye, J. Eberth, D. Fedorov, V.N. Fedosseev, L.M. Fraile, S. Franchoo, K. Gladnishki, D. Habs, K. Heyde, H. Huysse, O. Ivanov, J. Iwanicki, J. Jolie, B. Jonson, Th. Kröll, R. Krücken, O. Kester, U. Köster, A. Lagoyannis, L. Liljeby, G. Lo Bianco, B.A. Marsh, O. Niedermaier, T. Nilsson, M. Oinonen, G. Pascovici, P. Reiter, A. Saltarelli, H. Scheit, D. Schwalm, T. Sieber, N. Mirnova, J. Van De Walle, P. Van Duppen, S. Zemlyanoi, N. Warr, D. Weishaar, F. Wenander, *Coulomb Excitation of $^{68,70}\text{Cu}$: First Use of Postaccelerated Isomeric Beams*, Phys. Rev. Lett. **98**, 122701 (2007).
 33. <http://www.nndc.bnl.gov/nudat2/>
 34. V. Bondarenko, J. Honzatko, I. Tomandl, D. Bucurescu, T.v Egidy, J. Ott, W. Schauer, H.-F. Wirth, C. Doll, *Origin of the anomalous population of long-lived isomers in odd-A Te isotopes*, Phys. Rev. **C 60**, 027302 (1999).
 35. J.A. Dowell, A.R. Sancho, D. Anand, W. Wolf, *Noninvasive measurements for studying the tumoral pharmacokinetics of platinum anticancer drugs in solid tumors*, Adv. Drug Deliv. Rev. **41**, 111 (2000).
 36. M.J. Rivard, L.M. Bobek, R.A. Butler, M.A. Garland, D.J. Hill, J.K. Krieger, J.B. Muckerheide, B.D. Patton, E.B. Silberstein, *The US national isotope program: Current status and strategy for future success*, Appl. Rad. Isotopes, **63**, 157 (2005).
 37. A. Bishayee, D.V. Rao, S.C. Srivastava, L.G. Bouchet, W.E. Bolch, R.W. Howell, *Marrow-Sparing Effects of $^{117m}\text{Sn}(4+)\text{Diethylenetriaminepentaacetic Acid}$ for Ra-*

- dionuclide Therapy of Bone Cancer*, J. Nucl. Med. **41**, 2043 (2000).
38. B. Ponsard, S.C. Srivastava, L.F. Mausner, F.F.(Russ) Knapp, M.A. Garland, S. Mirzadeh, *Production of Sn-117m in the BR2 high-flux reactor*, Appl. Radiat. Isot. **67**, 1158 (2009).
 39. J. Raloff, *Desperately Seeking Moly*, ScienceNews **176**, 16 (2009).
 40. D.M. Lewis, *⁹⁹Mo supply—the times they are a-changing*, Eur. J. Nucl. Med. Mol. Imaging **36**, 1371 (2009).
 41. A.C. Apostolidis, R. Carlos-Marquez, W. Janssens, R. Molinet, T. Nikula, A. Ouadi, *Cancer treatment using Bi-213 and Ac-225 in radioimmunotherapy*, Nucl. News **44**, 29 (2001).
 42. A.C. Apostolidis, R. Molinet, J. McGinley, K. Abbas, J. Möllenbeck, A. Morgenstern, *Cyclotron production of Ac-225 for targeted alpha therapy*, Appl. Radiat. Isot. **62**, 383 (2005).
 43. O.D. Maslov, A.V. Sabel'nikov, S.N. Dmitriev, *Preparation of ²²⁵Ac by ²²⁶Ra(γ ,n) Photonuclear Reaction on an Electron Accelerator, MT-25 Microtron*, Radiochemistry **48**, 195 (2006).
 44. H. Uusijärvi, P. Bernhardt, F. Rösch, H.R. Maecke, E. Forsell-Aronsson, *Electron- and Positron-Emitting Radiolanthanides for Therapy: Aspects of Dosimetry and Production*, J. Nucl. Med. **47**, 807 (2006).
 45. N. Karavida and A. Notopoulos, *Radiation Synovectomy: an effective alternative treatment for inflamed small joints*, Hippokratia **14**, 22 (2010).
 46. F. Buchegger, F. Perillo-Adamer, Y.M. Dupertuis, A. Bischof Delaloye, *Auger radiation targeted into DNA: a therapy perspective*, Eur. J. Nucl. Med. **33**, 1352 (2006).
 47. C.J. Anderson and R. Ferdani, *Copper-64 Radiopharmaceuticals for PET Imaging of Cancer: Advances in Preclinical and Clinical Research* Cancer Biother. Radiopharmac. **24**, 379 (2009).
 48. D. Baltas, G. Lympelopoulou, E. Löffler, P. Mavroidis, *A radiobiological investigation on dose and dose rate for permanent implant brachytherapy of breast using I-125 or Pd-103 sources*, Medical Physics **37**, 2572 (2010).
 49. N. Jansen, J.M. Deneufbourg and P. Nickers, *Adjuvant stereotactic permanent seed breast implant: A boost series in view of partial breast irradiation*, Int. J. Rad. Oncology, Biology, Physics **67**, 1052 (2007).
 50. C. Grignon, J. Barbet, M. Bardies, T. Carlier, J.F. Chantal, O. Couturier, J.P. Cassonnet, A. Faivre, L. Ferrer, S. Gireault, T. Haruyama, P. Le Ray, L. Luquin, S. Lupone, C. Metivier, E. Morteau, N. Servagent, D. Thers, *Nuclear medical imaging using $\beta^+\gamma$ coincidences from ⁴⁴Sc radionuclide with liquid xenon as detector medium*, Nucl. Instr. Meth. **A 571**, 142 (2007).
 51. S. Hassfjell and M.W. Brechbiel, *The development of the α -particle emitting radionuclides ²¹²Pb and ²¹³Pb and their decay chain related radionuclides, for therapy applications*, Chem. Rev. **101**, 2019 (2001).
 52. Y. Miao, M. Hylarides, D.R. Fisher, T. Shelton, H. Moore, D.W. Wester, A.R. Fritzberg, C.T. Winkelmann, T. Hoffman, T.P. Quinn, *Melanoma Therapy via Peptide-Targeted α -Radiation*, Clin. Cancer Res. **11**, 5616 (2005).
 53. M.L.P. Antunes and M.N. Martins, *Two proton and two neutron photoemission cross sections of ⁶³Cu* Phys. Rev. **C52**, 1484 (1995).
 54. E. Garin, Y. Rolland, E. Boucher, V. Ardisson, S. Laffont, K. Boudjema, P. Bourguet, J.L. Raoul, *First experience of hepatic radioembolization using microspheres labelled with yttrium-90 (TheraSphere): practical aspects concerning its implementation*, Eur. J. Nucl. Med. Mol. Imaging **37**, 453 (2010).
 55. H.L. Ravn et al., patent WO2006074960 (2006).
 56. K. Abbas, S. Buono, N. Burgio, G. Cotogno, N. Gibson, L. Maciocco, C. Mercurio, A. Santagata, F. Simonelli, H. Tagziria, *Development of an accelerator driven neutron activator for medical radioisotope production*, Nucl. Instr. Meth. **A 601**, 223(2009) .
 57. S.H. Aaltonen, V.V. Kataja, T. Lahtinen, J.-E. Palmgren, T. Forsell, *Eight years experience of local prostate cancer treatment with permanent ¹²⁵I seed brachytherapy - Morbidity and outcome results*, Radiotherapy and Oncology **91**, 213 (2009).
 58. W. Ensinger, P. Vater, S. Heise, A. Moeslang, K. Schloesser, *Radioisotope ion implantation and ion beam mixing of cardiovascular stents for treatment of coronary artery diseases*, Surface and Coatings Technology **196**, 288 (2005).
 59. W. Assmann, M. Schubert, A. Held, A. Pichler, A. Chill, S. Kiermaier, K. Schlösser, H. Busch, K. Schenk, D. Streufert, I. Lanzl, *Biodegradable radioactive implants for glaucoma filtering surgery produced by ion implantation*, Nucl. Instr. Meth. **B 257**, 108 (2007).